Effect of Weak Reductant on Properties of Electroless Copper Polyacrylonitrile Nanocomposites for Electromagnetic Interference Shielding

Keng-Yu Tsao,[1] Chang-Cheng Chen,[1] Chi-Yuan Huang,[1] Ching-Shan Tsai,[1] Sung-Yeng Yang,[2] Jen-Taut Yeh,[3] Kan-Nan Chen[4]

[1]*Department of Materials Engineering, Tatung University, Taipei 10452, Taiwan*
[2]*Department of Chemical and Biochemical Engineering, Kao Yuan University, Kaohsiung County 82151, Taiwan*
[3]*Department of Polymer Engineering, National Taiwan University of Science and Technology, Taipei 10607, Taiwan*
[4]*Department of Chemistry, Tamkang University, Tamsui 25137, Taiwan*

Received 28 January 2010; accepted 13 March 2010
DOI 10.1002/app.32467
Published online 27 May 2010 in Wiley InterScience (www.interscience.wiley.com).

ABSTRACT: In this work, the electroless copper method with different reductant compositions ($NaHSO_3$/$Na_2S_2O_3{\cdot}5H_2O$ and $Na_2S_2O_3{\cdot}5H_2O$) without sensitizing and activating, was used to deposit copper-sulfide deposition on the polyacrylonitrile (PAN) surface for electromagnetic interference (EMI) shielding materials. The weak reductant, $NaHSO_3$, in the electroless copper method was used to control the phase of copper-sulfide deposition. The $Cu_{x(x=1-1.8)}S$ was deposited on the PAN (Cu_xS-PAN) by reductant composition ($NaHSO_3$/$Na_2S_2O_3{\cdot}5H_2O$) and the $Cu_{x(x=1-1.8)}S$ deposition of Cu_xS-PAN possesses three kinds of copper-sulfide phases (CuS, $Cu_{1.75}S$ and $Cu_{1.8}S$). However, the electroless copper with reductant was only $Na_2S_2O_3{\cdot}5H_2O$ (without weak reductant, $NaHSO_3$), the hexagonal CuS deposition was plated on the PAN (CuS-PAN) and increased the EMI shielding effectiveness of CuS-PAN composites about 10–15 dB. In this study, the best EMI SE of CuS-PAN and Cu_xS-PAN composites were about 27–30 dB and 15–17 dB respectively, as the cupric ion concentration was 0.24 *M*. The volume resistivity of CuS-PAN composite was about 1000 times lower than that of Cu_xS-PAN composite and lowest volume resistivity of CuS-PAN composites was 0.012 Ω cm, as the cupric ion concentration was 0.24 *M*. © 2010 Wiley Periodicals, Inc. J Appl Polym Sci 118: 936–942, 2010

Key words: EMI; electroless; CuS; polyacrylonitrile

INTRODUCTION

There is a rapidly increasing interest in the electromagnetic interference (EMI) shielding field for commercial and military use, as well as for scientific electrical products and electronic devices.[1] Electronic equipment should not emit electromagnetic waves which influence other devices. The common way to avoid EMI problems is to use materials with high conductivity, such as metals or conductive polymers as a shielding mechanism. When compared with metals, a polymer has such advantages as injecting formation, having various shapes, a better appearance, low cost and being lightweight. This is true, especially in many notably nonstructural applications, in which a mass decrease using plastics is desired.[2,3] Nevertheless, they are commonly used as electrical insulators and do not prevent the passage of electromagnetic waves. Therefore, conductive polymers now receive more attention for EMI shielding.[4,5] Many types of technology have been developed to provide EMI shielding. The techniques for plastic EMI shielding include electroless plating,[6] electroplating,[7] conductive paints,[7] conductive fillers filled composites,[8] intrinsic conductive polymers (ICPs),[9] and other metallization processes. Among them, electroless metal plating is probably a preferred way to produce metallization of polymer substrates. This method is based on the chemical reduction of metal ions in the solution to metallic atoms on the surface through a reducing agent in the solution, and is not constrained by shape, size or conductivity of the supporting substrate.[10] A conductive layer on the polymer surface increases the electron transport ability for polymer composites, and it reaches the EMI shielding ability.

Copper sulfides exist in a wide variety of compositions, ranging from copper-rich chalcocite (Cu_2S) to copper-deficient villamaninite (CuS_2) with other intermediate compounds, in-between, such as covellite (CuS), djurleite ($Cu_{1.95}S$), and anilite ($Cu_{1.75}S$), among others.[11] Chemical bath deposition has been extensively used for depositing copper sulfide films, usually named Cu_xS films.[12] Copper sulfides with copper vacancies in the lattice have been studied extensively for their application as p-type semiconductors material in metal-like electrical conductivity,[13] chemical-sensing

Correspondence to: C.-Y. Huang (cyhuang@ttu.edu.tw).
Contract grant sponsor: National Science Council; contract grant number: NSC 94-2216-E-036-015.

capability[14] and ideal characteristics for solar energy absorption.[15]

Most electroless copper methods deposit metal in alkaline bath. This method needs some activation and sensitization pretreatment and then the copper metal layer is oxygenated easily in the air.[10,16,17] In this study, the acid electroless copper method is used to deposit copper-sulfide deposition on the substrate for EMI shielding effectiveness (SE), and the copper-sulfide compound contains antioxidation in the air. The different reductant compositions, $NaHSO_3/Na_2S_2O_3{\cdot}5H_2O$ and $Na_2S_2O_3{\cdot}5H_2O$, deposit Cu_xS and CuS layer on the PAN surface, respectively. The CuS-PAN composites possess a better EMI SE than Cu_xS-PAN composites.

EXPERIMENTAL

Materials

Polyacrylonitrile (PAN) powders were obtained from Tong Hwa Synthetic and used as the substrate. The particles size of PAN powder is 1–10 μm, and has 93% of polyacrylontrile and (7%) vinyl acetate. The PAN powders were dissolved completely in dimethyformanide (DMF) to form PAN solution. Then the above PAN solution is poured into the Petri dish slowly. Firstly, it was dried to form the PAN film in an oven at 40°C. Secondly, in the process of making the residual solvent in the PAN film was vaporized. Then the film was dried in vacuum oven.

Electroless deposit

For composition and operation conditions of electroless copper bath, chemical composition of electroless copper bath and the abbreviations of composites are listed in Table I. The cupric sulfate ($CuSO_4{\cdot}5H_2O$), sodium thiosulfate ($Na_2S_2O_3{\cdot}5H_2O$), and sodium hydrogen sulfate ($NaHSO_3$) were produced by Nihon Shiyaku Industries. All the specimens were plated in the elecroless copper solution at 85°C for 1 hour and were stirred by nitrogen. After plating, the CuS-PAN and Cu_xS-PAN were washed with water until the surface was cleaned up and then dried in a vacuum oven.

EMI SE and resistivity measurement

The SE of the composite was measured by the method using the flanged circular coaxial transmission line holder. The range of frequencies measured in this equipment is from 1 MHz to 1.8 GHz.[18] This holder is similar to that of the circular coaxial transmission line holder. The dynamic rang of EMI SE was 90–100 dBm. The SE values of composites were obtained by taking out the background shielding measurement. However, the measurement frequency range list on ASTM D4935-99 is from 30 MHz to 1.5 GHz. The EMI SE is voltage dependent below the range of 30 MHz,[19] the testing frequency range of composites for EMI SE in this investigation is from 30 MHz to 1.5 GHz.[2] The volume electrical resistivity of copper-sulfide PAN composite was detected by HIOKI 3227 Megohmmeter. The measurement used a pair of copper clamping apparatuses, the distance of the clamping apparatuses was 1 cm, the range of voltage was 9 V (lower limit value) to 900 V (upper limit value) and the charge time was 20 s. The thickness of CuS-PAN and Cu_xS-PAN composites were measured by micrometer screw gauge (Mitutoyo MDC-25P), and the thickness range of sample were 0.050 to 0.076 mm.

TABLE I
The Abbreviations of Electroless Bath

	Components of electroless copper bath		
	$CuSO_4$–$5H_2O$ (*M*)	$NaHSO_3$ (*M*)	$Na_2S_2O_3$–$5H_2O$ (*M*)
PAN			
012NN	0.12	0.06	0.06
024NN	0.24	0.12	0.12
012N	0.12		0.06
024N	0.24		0.12

Field emission scanning electron microscope imaging

The surface morphology of copper-sulfide PAN composites were analyzed by field emission scanning electron microscope(FE-SEM HITACH IS-4800). The surface and cross-section morphology of specimens were viewed by FE-SEM at voltage 1.0 kv and 3.0 kv, respectively.

X-ray diffraction analysis

The X-ray Diffraction Pattern of copper-sulfide depositions were analyzed at room temperature by X-ray powder diffractometer (XRPD, Japan MAC Sience, MXP18) utilizing CuKα radiation of wavelength 1.54 Å. The scanning speed and sample width were 4.0°/min and 0.02° respectively. During electroless process a part of the copper-sulfide powder was synthesized in the electroless bath, without coating on the PAN film. The copper-sulfide powder was percolated and cleaned with deionized water, then dried in a vacuum oven. The high power X-ray diffractometer (HP-XRD, MAC Science, M 21X) was used to analyze the copper-sulfide powder at room temperature utilizing CuKα radiation of a wavelength at 1.54 Å. The scanning speed and sample width were 1.2°/

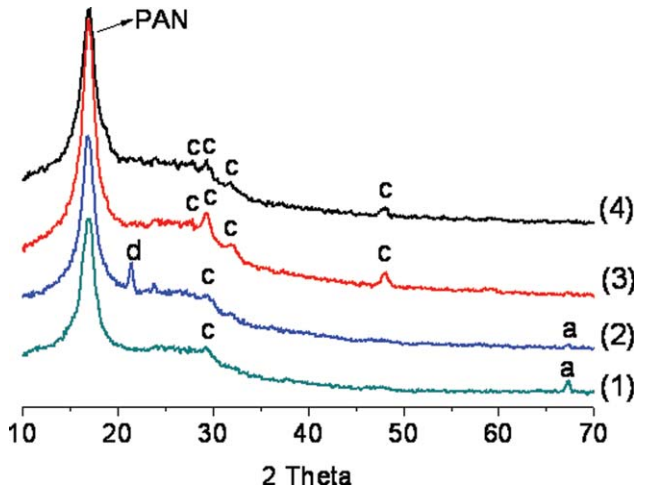

Figure 1 The GIA-XRD diffraction patterns of CuS-PAN and Cu_xS-PAN at various cupric ion concentrations as follow: (1) 012NN, (2) 024NN, (3) 012N, (4) 024N (peaks of covellite-c, anilite-a, digenite-d).

min and 0.02°, respectively. The composition and structure of the copper-sulfide deposition and powder were determined by the conventional 2Θ Bragg diffraction method.

RESULTS AND DISCUSSION

Composition analysis by x-ray diffraction

The X-ray diffraction pattern is used to check out the composition of copper-sulfide depositions. To avoid the influence of PAN substrate diffraction pattern, the grazing incident angle X-ray diffraction (GIA-XRD) is used to analyze the copper-sulfide deposition. The X-ray diffraction patterns of electroless plating copper-sulfide depositions are shown in Figure 1. The XRD pattern of 012N and 024N (reductant only $Na_2S_2O_3{\cdot}5H_2O$) composites show hexagonal CuS (covellite) characteristic peaks (Fig. 1, curve 3 and 4) at $2\Theta = 27.9$, 29.3, 31.7, and 48.0° from JCPDS files No. 06–0464.There are no characteristic XRD peaks arising from Cu_2S, $Cu_{1.8}S$ and $Cu_{1.75}S$. It indicated that the depositional layer is a pure phase of CuS. However, the XRD pattern of 012NN and 024NN (reductant composition $NaHSO_3/Na_2S_2O_3{\cdot}5H_2O$) composites show three kinds of Cu_xS crystal characteristic peaks (Fig. 1, curve 1 and 2), the crystal of hexagonal CuS (covellite) (peak at $2\Theta = 29.3°$), orthorhombic $Cu_{1.75}S$ (anilite) (peak at $2\Theta = 67.2°$) and $Cu_{1.8}S$ (digenite) (peak at $2\Theta = 21.4°$). Therefore, the deposition of 012NN and 024NN (reductant composition $NaHSO_3/Na_2S_2O_3{\cdot}5H_2O$) composites could have three kinds of copper-sulfide (Cu_xS, $x = 1$–1.8) phases in the depositional composites.

At room temperature, copper sulfide can form five stable phases[20]: covellite CuS, anilite $Cu_{1.75}S$, digenite $Cu_{1.8}S$, djurleite $Cu_{1.95}S$, and chalcocite Cu_2S. In this research, the different reductant compositions $NaHSO_3/Na_2S_2O_3{\cdot}5H_2O$ and $Na_2S_2O_3{\cdot}5H_2O$ are used to deposit the differnt copper-sulfide ($Cu_{x(x=1-1.8)}S$ and CuS) deposition respectively. The hexagonal CuS is produced by chemical reaction of $CuSO_4{\cdot}5H_2O$ and $Na_2S_2O_3{\cdot}5H_2O$ in water. The following equations[21] can represent the formation of CuS in this investigation:

$$Cu^{2+} + S_2O_3^{2-} + 2H_2O \longrightarrow [Cu(S_2O_3)(H_2O)_2]$$
$$[Cu(S_2O_3)(H_2O)_2] \longrightarrow CuS\downarrow + SO_4^{2-} + 2H^+ + H_2O$$
$$Cu^{2+} + 2S_2O_3^{2-} \rightarrow [Cu(S_2O_3)_2]^{2-}$$
$$[Cu(S_2O_3)_2]^{2-} + 6H_2O \rightarrow CuS\downarrow + 3SO_4^{2-} + 12H^+$$
$$n\,CuS \longrightarrow (CuS)_n$$

The CuS (covellite) with a hexagonal structure was also prepared by Tezuka et al.[12] with copper and sulfur ions reaction. In hexagonal structure, the copper ion is at the center combined with three sulfur ions in triangular groups on their bases to form sheets. These triangular groups lie in a plane between the tetragonal sheets.[11,22]

The ability of reductant gradually releases sulfide ions in acidic bath. The formation of Cu^+ ions could be attributed to the reduction of Cu^{2+} ions by the sulfide ions present in the bath. Thus, the presences of a series of Cu_xS phases are expected depending upon the experimental conditions.[23] The Cu (II) reduction process that suggests deposition at the electrode is written as:

$$Cu^{2+} + e^- \longrightarrow Cu^+$$

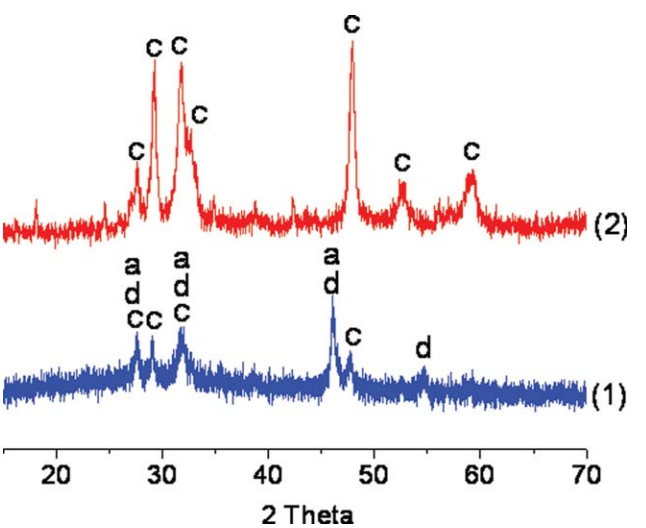

Figure 2 The HP-XRD diffraction patterns of 024NN (1) and 024N (2) copper-sulfide powder (peaks of covellite-c, anilite-a, digenite-d). [Color figure can be viewed in the online issue, which is available at www.interscience.wiley.com.]

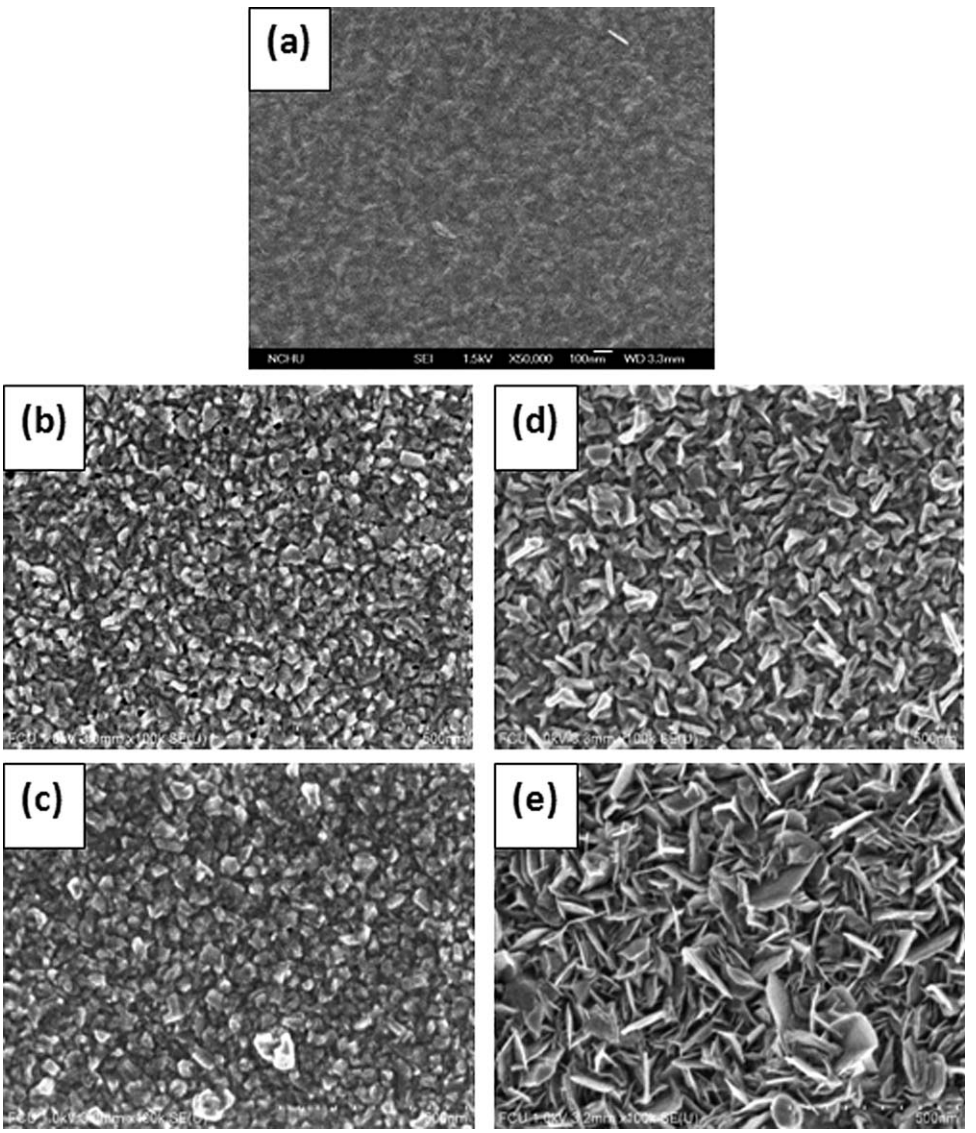

Figure 3 FE-SEM surface morphologies of CuS-PAN and Cu_xS-PAN at various cupric ion concentrations as follow: (a) PAN, (b) 012NN, (c) 024NN, (d) 012N, (e) 024N.

In this study, PAN film is without activation and sensitization pretreatment before using the electroless copper method. It is because that acrylonitrile group (—C≡N) of PAN possesses a very high polarity. This arises from the strong dipole moment of the nitrile groups. The lone pair orbital of nitrogen can engage in hydrogen bonding and electros in the π orbital of the nitrile triple bond which can interact with transition metal ions.[24]

During electroless process a part of the copper-sulfide powder was synthesized in the electroless bath, without coating on the PAN film. The high power X-ray diffraction (HP-XRD) is used to analyze the copper-sulfide powder, and the HP-XRD pattern is shown in Figure 2. The XRD pattern of 024N matches the hexagonal CuS (covellite) characteristic peaks (Fig. 2, curve 2) at $2\Theta = 27.66$, 29.26, 31.76, 47.90, 52.38, and 59.24° from JCPDS files No. 06–0464. However, the XRD pattern of 024NN is dissimilar 024N and the peaks appears at $2\Theta = 27.63$, 29.06, 31.74, 46.10, 47.73, and 54.68°, respectively. After comparing with the standard JCPDS file diffraction patterns, the crystalline microstructure of hexagonal CuS (JCPDS No. 06–0464), orthorhombic $Cu_{1.75}S$ (JCPDS No. 33–0489) and $Cu_{1.8}S$ (JCPDS No. 23–0962) are verified. The corresponding results of HP-XRD (Fig. 2) also proves the analysis of GIA-XRD (Fig. 1), and the reductant only $Na_2S_2O_3{\cdot}5H_2O$ deposit CuS on the PAN and the $Cu_{x(x=1-1.8)}S$ are deposited on the PAN by the reductant composition of $NaHSO_3$/ $Na_2S_2O_3{\cdot}5H_2O$.

Morphology of PAN coated copper-sulfide

In this study, the CuS and $Cu_{x(x=1-1.8)}S$ deposition are coated on the PAN film and the Field Emission

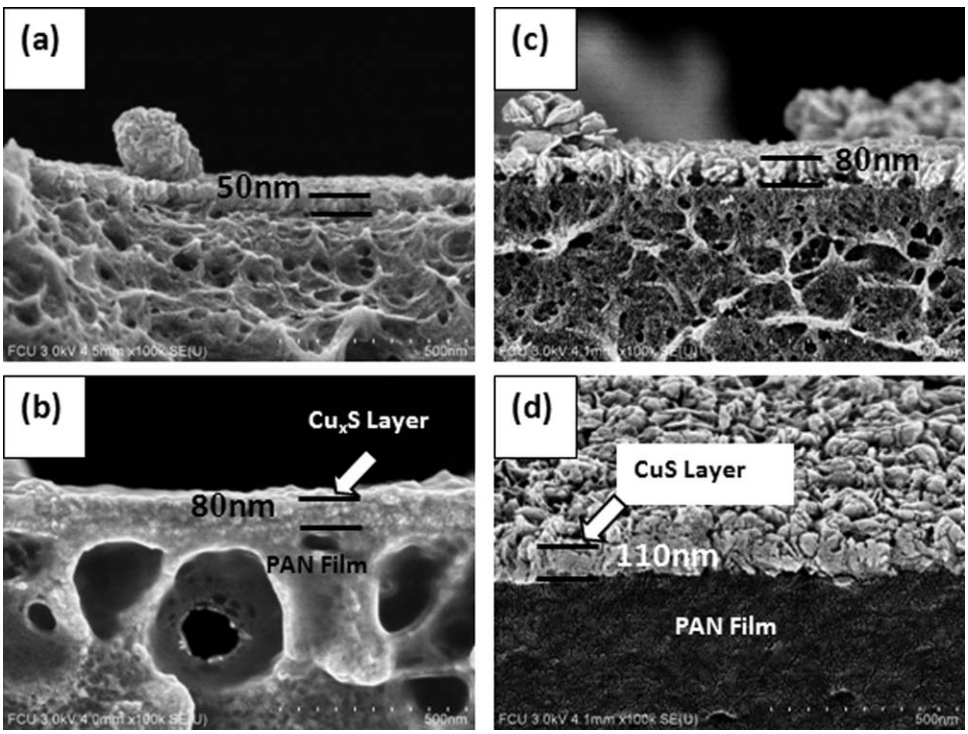

Figure 4 FE-SEM cross-section morphologies of CuS-PAN and Cu$_x$S-PAN at various cupric ion concentration as follow: (a) 012NN, (b) 024NN, (c) 012N, (d) 024N.

Scanning Electron Microscope (FE-SEM) morphology of CuS-PAN and Cu $_{x(x=1–1.8)}$S-PAN composites are shown in Figure 3. The smooth surface of PAN film is shown in Figures 3(a–e) and it indicates that the copper-sulfide deposition forms a regular and continuous base on the PAN film surface. The morphology of CuS and Cu$_{x(x=1–1.8)}$S depositions are different. The CuS grain formed a flake shape [Fig. 3(d,e)] and the Cu$_{x(x=1–1.8)}$S grain has a lumpy shape [Fig. 3(b,c)]. From the GIA-XRD analysis, the 012N and 024N (Fig. 1, curve 3 and 4) show hexagonal CuS characteristic peaks. Lindroos et al.[24] and Zhang et al.[25] also indicated that the flake grains shapes were a hexagonal CuS structure. In this investigation, when the cupric ion concentration is between 0.12 and 0.24 *M*, the average grain size of CuS and Cu$_x$S are to be listed below: 58.45 nm (012N), 77.06 nm (024N), 50.87 nm (012NN) and 50.67 nm (024NN). The CuS grain size of CuS-PAN is larger than that of Cu$_x$S-PAN, and the grain size of CuS increase with increasing cupric ion concentration. It is suggested that the pure phase CuS layer only has one of the copper-sulfide phases. Therefore, the CuS can grow with increasing cupric ion concentration. However, the Cu$_{x(x=1–1.8)}$S layer has three kinds of copper-sulfide phases which could affect the growth of Cu$_{x(x=1–1.8)}$S grain on each other and the grain size of Cu$_{x(x=1–1.8)}$S couldn't grow with increasing cupric ion concentration.

The FESEM micrograph of cross-section morphology of CuS-PAN and Cu$_x$S-PAN composites are shown in Figure 4. It is observed that the deposition thickness of CuS-PAN composites are higher than that of Cu$_x$S-PAN, and the average thickness of copper-sulfide layer plating on PAN film increases with increasing cupric ion concentration. The deposition thickness of 012N [Fig. 4(c)] and 024NN [Fig. 4(b)] are almost the same. Among of various compositions, 024N possesses the thickest CuS deposition; the thickness 105 nm is higher than the deposition thickness of other composites. The flake and lump shapes of the surface morphology (Fig. 3) are displayed evidently in the cross-section micrographs (Fig. 4).

EMI SE and resistivity analysis

The conductive copper-sulfide layer is coated onto the PAN surface and has mobile electricity carriers which interacted with the electromagnetic fields in the electromagnetic radiation. The copper-sulfide could be precipitated instantaneously from aqueous solutions of corresponding salts by the addition of Na_2S. A variety of Cu_2S, $Cu_{1.8}S$, $Cu_{1.4}S$ and CuS films were deposited by electroless chemical plating.[12,27] It is similar to this study for the application of EMI SE. The EMI SE of the CuS-PAN and Cu$_x$S-PAN composites manufactured in this study were measured between 30 MHz to 1500 MHz and plotted in Figure 5. The EMI SE of 012NN and 024NN increase without increasing cupric ion concentration and they are almost the same (about 15–17 dB).

Figure 5 shows that the EMI SE of CuS-PAN composites are better than those of Cu_xS-PAN composites, the EMI SE of 024N composite reaches 27∼30dB, 10∼15dB higher from Cu_xS-PAN (024NN). Han et al.[4] indicated that the thickness of conductive layer coating increased and consequently resulted in higher EMI SE. Figure 4 also shows that the 024N possesses the thickest thickness of CuS deposition. Luo et al.[27] also indicated that high conductive and dielectric constant of materials contribute to high EMI SE. In this investigation, the volume resistivities of CuS-PAN composites are lower than those of Cu_xS-PAN composites. The volume resistivity of various composites are shown in Figure 6. Figure 6 shows that 024N possesses the lowest resistivity of all composites. The volume resistivity of 024N is about 1000 times lower than that of 024NN and the 024N possesses the thickest CuS deposition (110 nm). Therefore, 024N shows the best EMI SE of all composites. In addition to 024N, the 012N has a lower resistivity than those of others (Fig. 6). According to the analysis of deposition thickness (Fig. 4), EMI SE (Fig. 5) and volume resistivity (Fig. 6), the EMI SE of 012N (CuS layer) is better than 024NN (Cu_xS layer) even though the thickness of 012N and 024NN are the same (80 nm). It is observed that the resistivity of CuS layer is lower than that of Cu_xS layer. Grozdanov et al.[11] also indicated that all films (Cu_2S, $Cu_{1.8}S$, $Cu_{1.4}S$, and CuS) displayed high electrical conductivity, with the CuS film being the most conductive. Hence, the affection of deposition composition (CuS/Cu_xS layer) is larger than that of deposition thickness for EMI SE. In this study, the main affection factor for EMI SE is deposition composition (CuS/Cu_xS layer); coating CuS layer on the PAN surface gets a better EMI SE than Cu_xS layer.

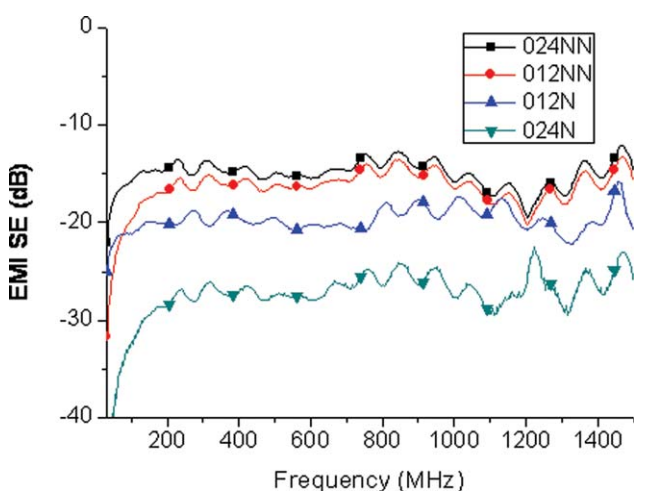

Figure 5 The EMI SE of CuS-PAN and Cu_xS-PAN composites. [Color figure can be viewed in the online issue, which is available at www.interscience.wiley.com.]

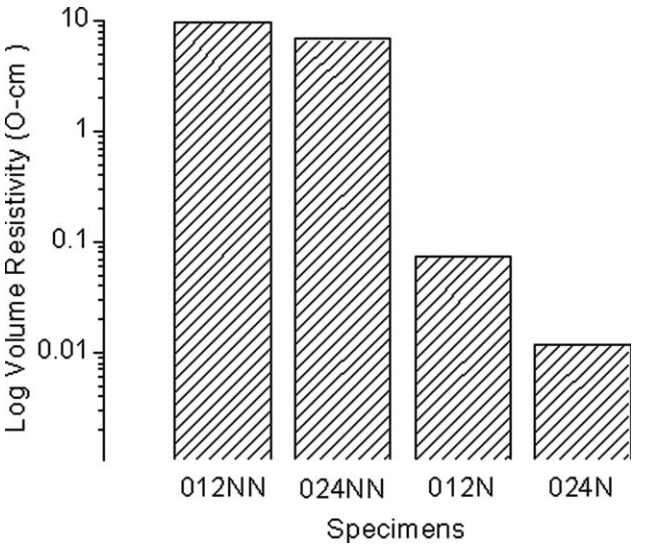

Figure 6 The log volume resistivity of CuS-PAN and Cu_xS-PAN composites.

CONCLUSIONS

The principle in achieving the significant EMI SE of the composite is always the same: good conductive layer and thickness of the conductive layer. In this study, the CuS-PAN and Cu_xS-PAN composites were prepared by applying electroless plating method without activation and sensitization pretreatment. The GIA-XRD and HP-XRD identifies that the composition of deposited layer is CuS and $Cu_{x(x=1-1.8)}S$ as the different reductant compositions $Na_2S_2O_3{\cdot}5H_2O$ and $NaHSO_3/Na_2S_2O_3{\cdot}5H_2O$ respectively. The deposited layer of CuS-PAN is a hexagonal CuS crystal and those of Cu_xS-PAN have three kinds of copper-sulfide phases (CuS, $Cu_{1.75}S$ and $Cu_{1.8}S$). The CuS grain size of CuS-PAN is larger than the Cu_xS grain size of Cu_xS-PAN, and the grain size of CuS increases with increasing cupric ion concentration. Generally, the EMI SE of CuS-PAN composites are better than those of Cu_xS-PAN composites, especially 024N, the EMI SE shows 27–30 dB, 10–15 dB higher from Cu_xS-PAN (024NN). In this investigation, the 024N possesses the best EMI SE of all composites. It is because the main affection factor for EMI SE is deposition composition in this study. The CuS deposition possesses a better electrical conductive than the Cu_xS deposition, and the 110 nm CuS thickness of 024N is higher than that of 012N (80 nm). Therefore, 024N shows the most advantages of all the EMI SE composites. With reductant $Na_2S_2O_3{\cdot}5H_2O$ and appropriate cupric ion concentration (0.24 *M*), the thick and CuS deposition composition is plated on the PAN and increases the EMI SE of about 60–75%.

The authors thank Tong-Hwa Synthetic Fiber Co., Ltd. for providing Polyacrylonitrile (PAN) powder.

References

1. Yuping, D.; Shunhua, L.; Hongtao, G. Sci Tech Adv Mater 2005, 6, 513.
2. Huang, C. Y.; Mo, W. W. Surf Coat Tech 2002, 154, 55.
3. Huang, C. Y.; Mo, W. W.; Roan, M. L. Surf Coat Tech 2004, 184, 123.
4. Han, E. G.; Kim, E. A.; Oh, K. W. Synth Met 2001, 123, 469.
5. Chen, C. C.; Hung, C. W.; Yang, S. Y.; Huang, C. Y. J Appl Polym Sci 2008, 109, 3679.
6. Huang, J. C. Adv Polym Tech 1995, 14, 137.
7. Huang, C. Y.; Mo, W. W.; Roan, M. L. Surf Coat Tech 2004, 184, 163.
8. Pomposo, J. A.; Rodriguez, J.; Grande, H. Synth Met 1999, 104, 107.
9. Lin, Y. M.; Yen, S. C. Appl Surf Sci 2001, 178, 116.
10. Tezuka, K.; Sheets, W. C.; Kurihara, R.; Shan, Y. J.; Imoto, H.; Marks, T. J.; Poeppelmeier, K. R. Solid State Sci 2007, 9, 95.
11. Grozdanov, I.; Najdoski, M. J. Solid State Chem 1995, 114, 469.
12. Mane, R. S.; Lokhande, C. D. Mater Chem Phys 2000, 65, 1.
13. Janata, J.; Josowicz, M.; Devaney, D. M. Anal Chem 1994, 66, R207.
14. Liao, X. H.; Chen, N. Y.; Xu, S.; Yang, S. B.; Zhu, J. J. J Cryst Growth 2003, 252, 593.
15. Mallory, G. O., Ed. J.B. Electroless Plating: Fundamentals and Applications; American Electroplaters and Surface Finishers Society: Orlando, 1990.
16. Ee, Y. C.; Chen, Z.; Chan, L.; See, A. K. H.; Law, S. B.; Tee, K. C.; Zeng, K. Y.; Shen, L. Thin Solid Films 2004, 197, 462.
17. Wilson, P. F.; Ma, M. T. IEEE Trans Electromagn Compact 1998, 30, 239.
18. Arnold, W. M.; Harris, P.; Partridge, C. A.; Andrews, M. K. IEEE Annual Report – Conference on Electrical Insulation and Dielectric Phenomena; San Francisco, 1996; 20 pp.
19. Sakamoto, T.; Sunamura, H.; Kawaura, H.; Hasegawa, T.; Nakayama, T.; Aono, M. Appl Phys Lett 2003, 82, 3032.
20. Zhang, Y. C.; Hu, X. Y.; Qiao, T. Solid State Commun 2004, 132, 779.
21. Xu, C.; Zhang, Z.; Ye, Q.; Liu, X. Chem Lett 2003, 32, 198.
22. Haram, K. S.; Mahadeshwar, A. R.; Dixit, S. G. J Phys Chem 1996, 100, 5868.
23. Henrici-Olive, G.; Olive, S. Adv Polym Sci 1979, 32, 125.
24. Lindroos, S.; Arnold, A.; Leskelä, M. Appl Surf Sci 2000, 158, 75.
25. Zhang, H. T.; Wu, G.; Chen, X. H. Mater Chem Phys 2006, 98, 298.
26. Grozdanov, I. Appl Surf Sci 1995, 84, 325.
27. Luo, X. C.; Chung, D. D. L. Compos Part B 1999, 30, 227.